OPEN ACCESS

International Journal of Innovations in Science & Technology

Effect of Concentration Variation on Zirconium Nickel Cobalt Metal Organic Framework-Based Electrode Material

Meishaar Hussain, Sidra Khalid*, Saira Shaheen, Sidra Ashraf, Hassan Shehzad, Joun Ali Faraz, Taimoor

Department of Physics, School of Science, University of Management and Technology, Lahore 54782, Pakistan

*Correspondence: sidra.khalid@umt.edu.pk

Citation | Hussain. M Khalid. S Shaheen. S Ashraf. S Shehzad H, Faraz. J. A., Taimoor, "Effect of Concentration Variation on Zirconium Nickel Cobalt Metal Organic Framework Based Electrode Material", IJIST, Vol. 07 Special Issue pp 30-37, July 2025

Received| April 29, 2025 **Revised|** May 25, 2025 **Accepted|** July 01, 2025 **Published|** July 05, 2025.

In this research, two samples of a ZrNiCo ZIF-67 with the change in molar concentration of metal to linker (1:1 and 1:2) were synthesized via the co-precipitation method. Then electrode fabrication was done. An attractive candidate for supercapacitor electrodes, ternary metal oxides ZIF 67 exhibit several desirable properties, including a large surface area, porosity, chemical stability, tailoring ability, redox activity, and low environmental impact. The porous polyhedral structure of ZrNiCo ZIF-67, which incorporates connected nanoparticles of varied compositions, greatly enhances the charge storage capacity. They are essential to a robust and sustainable energy future, and they have social, ecological, and economic significance. Electrochemical methods such as cyclic voltammetry (CV), galvanostatic charge and discharge (GCD), and electrochemical impedance spectroscopy (EIS) are among the various characterizations used to assess the electrode's performance. Other approaches include X-ray diffraction to study the crystal structure. With a specific capacitance of 232 F/g at a current density of 1 A/g, the ZrNiCo ZIF-67 (1:2) electrode material performs better than the other ZrNiCo ZIF-67 (1:1) materials. In order to create nanocomposites ZrNiCo ZIF-67 (1:2) with improved electrochemical characteristics, this research provides an easy and practical method. These materials can then be used as electrodes in supercapacitors for high specific capacitance.

Keywords: Zrnico Zif-67, Co-Precipitation Method, X-Ray Diffraction (XRD), Electrode Fabrication, Redox Activity, Electrochemical Performance

Introduction:

Emerging as a transforming discipline in material science, nanotechnology provides atomic and molecular level manipulation of matter. Thanks to this development, new materials with improved surface area, chemical stability, and customized features necessary for contemporary commercial and scientific uses [1][2][3] have become possible. Among its several contributions, nanotechnology is especially important for the creation of improved energy storage systems in which device efficiency is directly influenced by material performance at the nanoscale.

Prominent electrochemical energy storage devices with great interest due to their high-power density, fast charge-discharge capabilities, and long cycle life are supercapacitors, often referred to as ultracapacitors [4]. Supercapacitors' higher electrode surface area and electrochemical activity help them to store far more energy than conventional capacitors [5]. Faster energy transfer is made possible by their mechanisms, which either employ electrical double-layer capacitance or pseudo-capacitance, allowing for better than standard batteries [6][7]. Still, a major difficulty in supercapacitor research, meanwhile, is raising energy density while preserving high power density.

Recent research aimed at addressing this restriction has concentrated on the creation of sophisticated electrode materials such as ternary metal oxides. Comprising three separate metal components, these materials provide synergistic benefits, improving structural stability, redox activity, and electrical conductivity during cycling [8]. Improving the electrochemical performance and endurance of supercapacitor electrodes depends on such features.

A subfamily of metal-organic frameworks recognized for their tunable porosity, chemical robustness, and high surface area, zeolitic imidazolate frameworks (ZIFs) present one exciting class of precursors for these advanced materials [9][10][11]. Particularly, ZIF-67, consisting of cobalt ions and 2-methylimidazolate linkers, has shown promise as a precursor for producing porous metal oxides via ligand exchange or thermal decomposition [12][13][14]. Together with its capacity to host several metal species and structural similarity to ZIF-67 to ZIF-8, ZIF-67 is a flexible template for creating nanostructured compositions.

Incorporating zirconium (Zr) and nickel (Ni) into the ZIF-67 framework allows one to synthesize ZrNiCo-based composites with enhanced redox behaviour, electrochemical stability, and ion diffusion capacity [14]. These ternary composites not only preserve the great surface area and porosity of the original framework but also add several redox-active sites that help to increase specific capacitance.

This work intends to produce and describe ZrNiCo ZIF-67 composites with two different molar ratios (1:1 and 1:2) of metal to organic linker. The structural and electrochemical characteristics of the resulting materials are methodically assessed using X-ray diffraction (XRD), cyclic voltammetry (CV), galvanostatic charge–discharge (GCD), and electrochemical impedance spectroscopy (EIS) following a co-precipitation method followed by annealing. The aim is to find a composition that provides the best performance for supercapacitor uses and to know how molar ratio modification affects electrode behaviour.

Literature / Discussions:

Author mentioned that Supercapacitor (SC) technology is built on the work of Helmholtz, who established in 1853 that electrical charges may be held on both the surface of a conductor and the electrode-electrolyte "double-layer" interface. Shortly a century after, General Electric and Sohio (Standard Oil Company) published a lot of papers and patents [15]. Mostly, studies using electrodes for batteries and carbon-based fuel cells produced these first results. More broadly, they made it possible for nanotechnology to emerge, which in turn allowed surface area to grow and tailored nano-sized morphologies to be exploited. The energy and power densities of a system of energy storage devices characterize it essentially. Linking conventional capacitors with fuel cells, SCs are vital. While fuel cells fast store energy fast, traditional capacitors have a high-power density. Supercapacitors show more capacitance than conventional capacitors because of their larger surface areas of electrodes. Moreover, SCs can generate more power than batteries since their approaches to energy accumulation differ greatly. Unlike batteries, where the reverse is true, SCs have a surface-based rather than bulk-based charge-accumulating process. Following an explanation of how supercapacitors operate and an assessment of the technology's performance, the chapter notes the main conclusions in the area while also monitoring the technology's evolution over the years and trying to offer a useful classification [15].

Author in another study, explores how the nanomorphology of ZIFs greatly influences, even improves, the chemical properties of metal-organic compounds. Nanosized rhombic dodecahedral ZIF-67 crystals were synthesised easily at room temperature, co-precipitated, and subsequently extensively characterized by XRD, FT-IR, DRS, XPS, TEM, SEM, TGA, and N2/CO2 sorption investigations. Under mild reaction conditions, the as-prepared ZIF-67 material was found to be an effective heterogeneous co-catalyst for the photocatalytic reduction of CO2 by means of a ruthenium-based dye as a photosensitizer. With catalytic performance that is, 37.4 moles of CO per 30 minutes,the photocatalytic CO2 reduction system exceeded other types of MOFs when the reaction circumstances were just correct. The carbon source of the investigated CO was confirmed by isotope analysis of 13CO2. Furthermore, examined in the reaction system were the stability and reusability of the ZIF-67 co-catalyst. This work clarifies unexplored paths for the construction of photocatalytic nanoscale ZIF materials [14][16].

Objectives:

Using two molar ratios (1:1 and 1:2), co-precipitation allows one to synthesize ZrNiCo ZIF-67 composites.
To create and validate electrodes from the produced materials.
To evaluate their electrochemical performance.

Novelty:

The structure and electrochemical characteristics of ZrNiCo ZIF-67 composites are investigated in this work concerning changing the metal-to-linker molar ratio. Unlike earlier studies, it investigates two different stoichiometries to show how composition influences capacitance and charge transfer resistance. Within a ZIF-67 framework, the ternary combination of Zr, Ni, and Co provides improved redox activity and energy storage potential.

Methodology:

Room temperature co-precipitation was used to synthesize ZIF-67. To make a pink solution, specifically 0.9599 g of cobalt nitrate hexahydrate $[Co\ (NO_3)\ _2\cdot 6H_2O]$ was dissolved in 40 mL of deionized water and agitated for 30 minutes. To get a transparent solution, separately, 2.1014 g of benzene tricarboxylic acid was dissolved in another 40 mL of deionized water. Before the benzene tricarboxylic acid solution was added dropwise, the cobalt-containing solution was swirled for another 15 minutes. The reaction mixture was left at room temperature undisturbed for 24 hours. Collected by filtration, a purple solid precipitate was rinsed with deionized water and ethanol; it was dried at 80°C for twelve hours. This process produces a highly porous and single-metal cobalt-based ZIF-67 framework.

ZrNiCo ZIF-67 composites synthesized included nickel and zirconium in addition to cobalt into the ZIF structure. Two sets of samples were generated with varying metal-to-linker molar ratios. Dissolved in 80 mL of deionized water, 0.9596 g of cobalt nitrate hexahydrate, 0.9599 g of nickel nitrate hexahydrate, and 0.7697 g of zirconyl nitrate, sample 1 (1:1 ratio) was well homogeneous after vigorous stirring.

The identical mass of metal precursors was dissolved in 80 mL of deionized water, but the molar ratio of metal to linker was changed to 1:2 by changing the linker quantity. Both combinations allow for reaction at room temperature. The resultant particles were gathered by centrifugation, washed using deionized water and ethanol, and dried overnight at 80°C. Most importantly, the dried powders underwent two hours of thermal treatment at 800°C in a nitrogen environment under a ramp rate of 3°C/min. This calcination process converted as-synthesized precursors into redox-active sites and increased the structural integrity of electroactive ternary metal oxide nanocomposites.

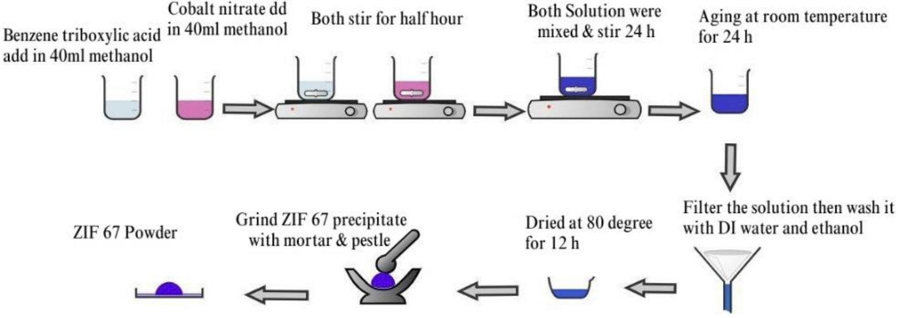

Figure 1. Schematic representation of the synthesis of pure cobalt-based ZIF-67 framework.

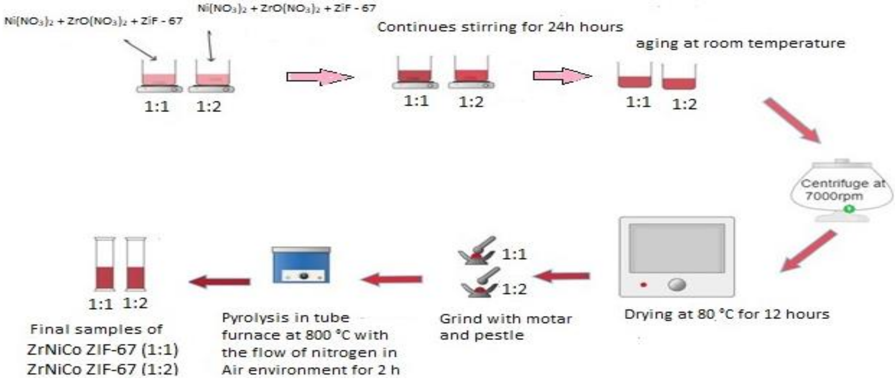

Figure 2. Schematic illustration of the synthesis process for ZrNiCo ZIF-67 composite materials with two different molar ratios (1:1 and 1:2) of metal precursors to organic linker.

For making functional electrodes, Deionized water, acetone, and alcohol were used to clean the nickel foam. The NMP solution was fortified with 80:10:10 weight ratios of electrode Redox-active material, binder (PVDF), and carbon black. Deionized water (DIW) was supplemented with 2 milligrams of the produced substance and 10 microliters of Nafion solution. The technique of making functional electrodes involved making a slurry, coating it onto nickel bubbles that were 1 cm by 1 cm in size, and then vacuum drying them at 110 °C for about 10 hours. Submerging the constructed cell in a 3M KOH electrolyte solution completes the assembly process. Then the Teflon cap and platinum coil were placed on top of it. The built electrode was immersed in the cylindrical cell to serve as a working electrode, while an Ag/AgCl electrode served as a reference electrode. The electrochemical workstation consisted of three interconnected electrodes.

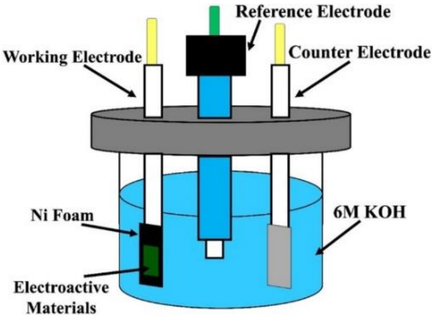

Figure 3. Schematic diagram for the three-electrode electrochemical cell arrangement utilized for characterization. A platinum counter electrode, an Ag/AgCl reference electrode, and a working electrode.

Characterization Techniques:

This is a collection of techniques used to determine the composition and electrical properties of man-made materials.

X-ray Diffraction
CV
GCD
EIS

Results and Discussion:

X-Ray Diffraction (XRD) Analysis:

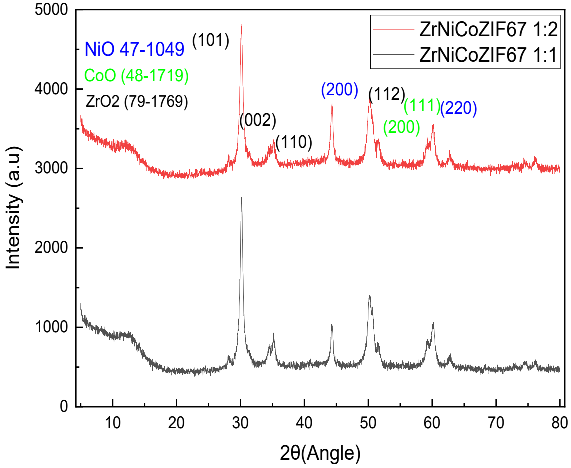

Figure 4. X-ray diffraction (XRD) patterns of ZrNiCo ZIF-67 composites with 1:1 and 1:2 molar ratios of metal to linker.

Two alternative molar ratios (1:1 and 1:2) were used in X-ray diffraction examination to determine the crystalline structure and phase composition of the produced ZrNiCo ZIF-67 composites. As Figure 4 shows, both samples show separate peaks matching the crystalline phases of ZrO_2, NiO, and CoO. Complementing the standard reference pattern (JCPDS 39-1346), the diffraction peaks at 2θ values of 30.01°, 34.92°, 38.6°, and 50.02° correspond to the (101), (002), (110), and (112) planes of rhombohedral ZrO_2. Likewise, NiO peaks seen at 43.3° and 62.9° correspond to the (200) and (220) planes of its cubic phase (JCPDS 47-1049). Consistent with JCPDS 48-1719, CoO displayed peaks at 54.88° and 60° corresponding to the (111) and (200) planes. These results validate that the ternary composite preserves the unique crystal properties of every metal oxide component. Although changing the metal-to-linker ratio does not appreciably affect the crystallographic phases, the relative intensities indicate variations in crystallinity and phase dominance, which perhaps influence electrochemical performance in both samples.

GCD Galvanostatic Charge-Discharge Analysis:

To assess the composites' capacitive behaviour, GCD measurements were performed in a three-electrode setup within a 3M KOH electrolyte. Overall, investigated current densities (2–100 A/g), the ZrNiCo ZIF-67 (1:2) electrode has a longer discharge duration, as shown in Figure 5.0, than its 1:1 counterpart. For the 1:2 sample, the specific capacitance computed peaked at 180 F/g at 1 A/g.

The 1:2 composite's longer discharge time points to enhanced energy storage capacity, most likely from a more developed mesoporous structure and increased availability of redox-active sites. Common behavior ascribed to inadequate electrolyte ion penetration at higher current rates is the reduction in specific capacitance with increasing current density observed in both specimens. Still, both electrodes kept good charge-discharge reversibility, suggesting structural durability during electrochemical cycling.

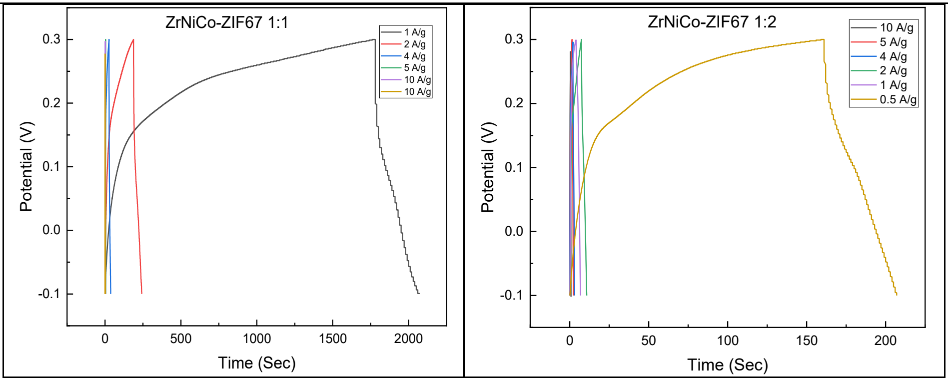

Figure 5. Galvanostatic charge-discharge (GCD) profiles of ZrNiCo ZIF-67 composites (1:1 and 1:2) recorded at various current densities.

Cyclic voltammetry (CV) Analysis:

Cyclic voltammetry was then used to examine the composites' further electrochemical characteristics. Under scan rates ranging from 2 to 100 mV/s, CV curves were collected in a potential range spanning -0.3 V to +0.3 V (vs. Ag/AgCl). Figure 6.0 shows both materials displaying quasi-rectangular CV profiles with separate redox peaks, hence demonstrating pseudocapacitive behavior.

Suggesting more electrochemical activity and capacitance, ZrNiCo ZIF-67 (1:2) showed a notably bigger integrated area and higher peak current among the two. At a two mV/s scan rate, the greatest specific capacitance of 232 F/g was attained. The ideal ratio of metal ions helps electron transmission and raises the density of electroactive sites, thereby explaining this improved performance. A decrease in capacitance was noted when scan rates rose, mostly from the limited diffusion of ions at faster speeds, therefore limiting deeper use of the electrode surface.

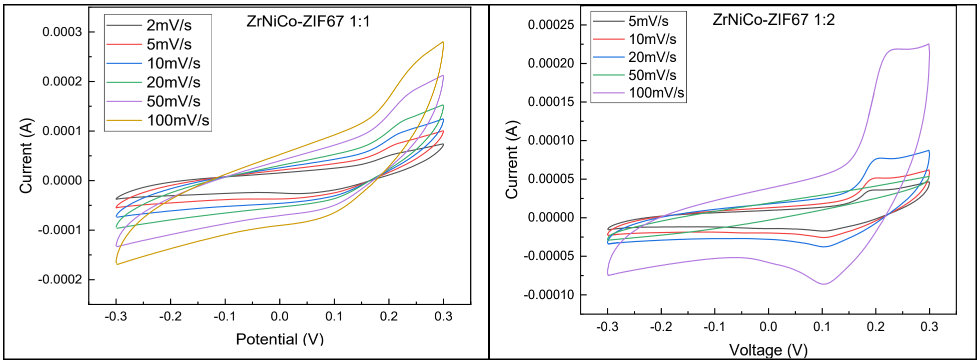

Figure 6 Cyclic voltammetry (CV) curves of ZrNiCo ZIF-67 composites (1:1 and 1:2) measured across scan rates from 2 to 100 mV/s.

Electrochemical Impedance Spectroscopy (EIS) Analysis:

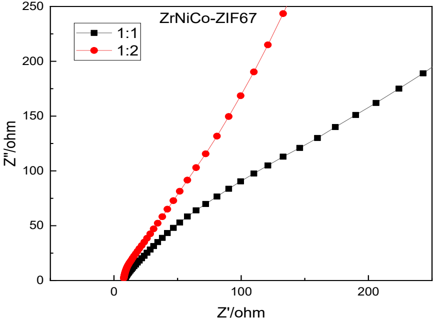

Figure 7. Electrochemical impedance spectroscopy (EIS) Nyquist plots of ZrNiCo ZIF-67 composites (1:1 and 1:2). The smaller semicircle for the 1:2 sample reflects lower charge transfer resistance, suggesting better electrical conductivity and ion diffusion.

EIS studies spanning a frequency range of 10^2 to 10^5 Hz allowed one to examine charge transfer resistance and ion diffusion kinetics. Representing charge transfer resistance (Rct), the Nyquist plots in Figure 7.0 show a straight line in the low-frequency region and a semi-circular arc in the high-frequency region, suggesting Warburg impedance linked with ion diffusion.

Compared to 8.6 Ω for the 1:1 sample, the smaller semicircle diameter of the ZrNiCo ZIF-67 (1:2) composite corresponded to a lower Rct value of 7.3 Ω. In the 1:2 electrode, this decrease in resistance corresponds with higher electron mobility and improved electrical conductivity. Moreover, the steeper slope in the low-frequency part of the 1:2 sample guarantees enhanced capacitive behavior and ion transport. The optimal stoichiometric balance of metals and linkers helps to explain these developments in more efficient electrolyte accessibility and greater connection among active particles.

Conclusions:

Nanocomposites of ternary metal oxides ZrNiCo ZIF-67 were produced through the use of a co-precipitation process with the change of molar concentration (1:1 and 1:2). By using X-ray diffraction, the crystal structures of the composites were analyzed. With its high-rate capacity and outstanding specific capacitance, the ZrNiCo ZIF-67 (1:2) hybrid nanocomposite shows significant promise as a material for supercapacitor electrodes. The specific capacitance of this electrode material, which contains connected nanoparticles, was 232F/g, and it showed an enhanced capacitance when tested at a scan rate of 2mv/s. The EIS study also shows that the ohmic resistance value is lower (Rs = 7.3 Ω) than other electrode materials, which means that the electrical conductivity and charge transfer rate are better. This method is useful for supercapacitors and other high-performance, practically applicable energy storage devices.

References:

[1] Y. W. Shiza Malik, Khalid Muhammad, "Nanotechnology: A Revolution in Modern Industry," *Molecules*, vol. 28, no. 2, p. 661, 2023, doi: https://doi.org/10.3390/molecules28020661.

[2] H. Goesmann and C. Feldmann, "Nanoparticulate Functional Materials," *Angew. Chemie Int. Ed.*, vol. 49, no. 8, pp. 1362–1395, Feb. 2010, doi: 10.1002/ANIE.200903053.

[3] I. W. Hamley, "Nanotechnology with Soft Materials," *Angew. Chemie Int. Ed.*, vol. 42, no. 15, pp. 1692–1712, Apr. 2003, doi: 10.1002/ANIE.200200546.

[4] M. A. A. Abdul Ghani Olabi, Qaisar Abbas, Ahmed Al Makky, "Supercapacitors as next generation energy storage devices: Properties and applications," *Energy*, vol. 248, p. 123617, 2022, [Online]. Available: https://www.sciencedirect.com/science/article/abs/pii/S0360544222005205?via%3Dihub

[5] Y. M. Volfkovich, "Electrochemical Supercapacitors (a Review)," *Russ. J. Electrochem. 2021 574*, vol. 57, no. 4, pp. 311–347, May 2021, doi: 10.1134/S1023193521040108.

[6] S. A. J. Pranoti H. Patil, Vidya V. Kulkarni, "An Overview of Recent Advancements in Conducting Polymer–Metal Oxide Nanocomposites for Supercapacitor Application," *J. Compos. Sci*, vol. 6, no. 12, p. 363, 2022, doi: https://doi.org/10.3390/jcs6120363.

[7] S. W. J. Yedluri Anil Kumar, Nipa Roy, Tholkappiyan Ramachandran, Mohamed Hussien, Md Moniruzzaman, "Shaping the future of energy: The rise of supercapacitors progress in the last five years," *J. Energy Storage*, vol. 98, p. 113040, 2024, doi: https://doi.org/10.1016/j.est.2024.113040.

[8] T. H. Noor Tahir, Muhammad Zahid, Ijaz Ahmad Bhatti, Asim Mansha, Syed Ali Raza Naqvi, "Chapter 7 - Metal oxide-based ternary nanocomposites for wastewater

treatment," *Aquananotechnology*, pp. 135–158, 2021, doi: https://doi.org/10.1016/B978-0-12-821141-0.00022-7.

[9] S. Kouser, A. Hezam, M. J. N. Khadri, and S. A. Khanum, "A review on zeolite imidazole frameworks: synthesis, properties, and applications," *J. Porous Mater.*, vol. 29, no. 3, pp. 663–681, Jun. 2022, doi: 10.1007/S10934-021-01184-Z/METRICS.

[10] H. L. Ke Li, Nicholas Miwornunyuie, Lei Chen, Huang Jingyu, Paulette Serwaa Amaniampong, Desmond Ato Koomson, David Ewusi-Mensah, Wencong Xue, Guang Li, "Sustainable Application of ZIF-8 for Heavy-Metal Removal in Aqueous Solutions," *Sustainability*, vol. 13, no. 2, p. 984, 2021, doi: https://doi.org/10.3390/su13020984.

[11] S. S. A. S. Muhammad Altaf Nazir, Sami Ullah, Muhammad Umar Shahid, Ismail Hossain, Tayyaba Najam, Mostafa A. Ismail, Aziz ur Rehman, Md Rezaul Karim, "Zeolitic imidazolate frameworks (ZIF-8 & ZIF-67): Synthesis and application for wastewater treatment," *Sep. Purif. Technol.*, vol. 356, p. 129828, 2025, doi: https://doi.org/10.1016/j.seppur.2024.129828.

[12] R. L. & S. H. Wen-Long Xue, Pascal Kolodzeiski, Hanna Aucharova, Suresh Vasa, Athanasios Koutsianos, Roman Pallach, Jianbo Song, Louis Frentzel-Beyme, "Highly porous metal-organic framework liquids and glasses via a solvent-assisted linker exchange strategy of ZIF-8," *Nat. Commun.*, vol. 15, no. 4420, 2024, doi: https://doi.org/10.1038/s41467-024-48703-5.

[13] M. M. Zahra Ebrahimi, Mohammad Rad, Vahid Safarifard, "Solvent-assisted ligand exchange as a post-synthetic surface modification approach of Zn-based (ZIF-7, ZIF-8) and Co-based (ZIF-9, ZIF-67) zeolitic frameworks for energy storage application," *J. Mol. Liq.*, vol. 364, p. 120018, 2022, doi: https://doi.org/10.1016/j.molliq.2022.120018.

[14] S. Bibi, E. Pervaiz, and M. Ali, "Synthesis and applications of metal oxide derivatives of ZIF-67: a mini-review," *Chem. Pap.*, vol. 75, no. 6, pp. 2253–2275, Jun. 2021, doi: 10.1007/S11696-020-01473-Y/METRICS.

[15] R. C. and Y. K. Bharti, Ashwani Kumar, Gulzar Ahmed, Meenal Gupta, Patrizia Bocchetta, Ravikant Adalati, "Theories and models of supercapacitors with recent advancements: impact and interpretations," *Nano Express*, vol. 2, no. 2, 2021, doi: 10.1088/2632-959X/abf8c2.

[16] L. Z. Zhaoying Di, Runduo Zhang, Xiaonan Guo, Hanxiao Shen, Sebastien Royer, Jingbo Jia, Ying Wei, Yaping Li, "Efficiently catalytic purification of indoor formaldehyde upon Co-N sites derived from ZIF-67 carbonization," *Fuel*, vol. 380, p. 133152, 2025, doi: https://doi.org/10.1016/j.fuel.2024.133152.